Self-consistent electronic structure of multiquantum vortices in superconductors at $T \ll T_c$

2013 J. Phys.: Condens. Matter 25 225702

(http://iopscience.iop.org/0953-8984/25/22/225702)

J. Phys.: Condens. Matter **25** (2013) 225702 (10pp) doi:10.1088/0953-8984/25/22/225702

Self-consistent electronic structure of multiquantum vortices in superconductors at $T \ll T_c$

M A Silaev[1] **and V A Silaeva**[2]

[1] Institute for Physics of Microstructures, Russian Academy of Sciences, N Novgorod, 603950, Russia
[2] National Research University Higher School of Economics, 25/12 Bolshaja Pecherskaja street, Nizhny Novgorod 603155, Russia

E-mail: msilaev@ipm.sci-nnov.ru

Received 24 January 2013, in final form 8 April 2013
Published 15 May 2013
Online at stacks.iop.org/JPhysCM/25/225702

Abstract
We investigate the multiquantum vortex states in a type-II superconductor in both 'clean' and 'dirty' regimes defined by impurity scattering rate. Within a quasiclassical approach we calculate self-consistently the order parameter distributions and electronic local density of states (LDOS) profiles. In the clean case we find the low temperature vortex core anomaly predicted analytically by Volovik (1993 *JETP Lett.* **58** 455) and obtain the patterns of LDOS distributions. In the dirty regime multiquantum vortices feature a peculiar plateau in the zero energy LDOS profile, which can be considered as an experimental hallmark of multiquantum vortex formation in mesoscopic superconductors.

(Some figures may appear in colour only in the online journal)

1. Introduction

Modern technology development provides a unique possibility to study superconducting states at the nanoscale. Recently there has been much experimental effort focused on the investigation of exotic vortex states in mesoscopic superconducting samples of the size of several coherence lengths [1, 2]. Magnetic field can penetrate the sample in the form of a polygon-like vortex molecule, or individual vortices can merge forming a multiquantum giant vortex state with a winding number larger than unity [3]. The latter possibility is of particular interest, and the search for giant vortices in mesoscopic superconductors has been performed by means of various experimental techniques including transport measurements [4, 5], Bitter decoration [6], magnetometry [7], and scanning Hall probe experiments [8]. Currently much effort is invested in studies of nanoscale superconducting samples with the help of scanning tunneling microscopy (STM) techniques [9, 10], which have been achieved only recently and allow for a direct probe of the structure of vortex cores through measurement of the electronic local density of states (LDOS) distribution modified by vortices.

Such STM measurements have been proven to be an effective tool for experimental study of electronic structure of vortices in bulk superconductors [11–15]. Indeed, for temperatures much lower than the typical energy scale in superconductors $T \ll T_c$ the local differential conductance of the contact between the STM tip and superconductor as a function of voltage V is given by

$$\frac{dI}{dV}(V) = \frac{dI}{dV}_N \frac{N(\mathbf{r}, E = eV)}{N_0} \quad (1)$$

where $(dI/dV)_N$ is the conductance of the normal metal junction and N_0 is the electronic density of states at the Fermi level. The observation of zero-bias anomalies of tunneling conductance at the center of singly quantized vortices [11, 13, 12, 14, 15] clearly confirms the existence of bound vortex core states predicted by Caroli, de Gennes and Matricon (CdGM) [16]. In clean superconductors for each individual vortex the energy $\varepsilon(\mu)$ of a subgap electronic state varies from $-\Delta_0$ to $+\Delta_0 = \Delta(r = \infty)$ as one changes the angular momentum μ defined with respect to the vortex axis. At small energies $|\varepsilon| \ll \Delta_0$ the spectrum is a linear function of μ:

$$\varepsilon(\mu) = \omega\mu. \quad (2)$$

Here $\omega \sim \Delta_0/(k_F\xi)$, where $\xi = \hbar V_F/\Delta_0$ is coherence length, k_F is Fermi momentum and V_F is Fermi velocity. The wave functions of subgap states with spectrum (2) are localized inside vortex cores because of the Andreev reflection of quasiparticles from the core boundaries, and form the low energy LDOS singularity at the vortex center.

In multiquantum vortices with the winding number M the spectrum of electronic states contains M anomalous branches degenerate by electronic spin [17–21]:

$$\varepsilon_j(\mu) = \omega_j(\mu - \mu_j), \tag{3}$$

where $\omega_j \sim \Delta_0/(k_F\xi)$ and index j enumerates different spectral branches $(1 < j < M)$, $-k_F\xi \lesssim \mu_j \lesssim k_F\xi$. Each anomalous branch intersects the Fermi level and contributes to the low energy LDOS. The spectrum of localized electronic states in mesoscopic superconductors with several vortices has been shown to be very sensitive to the mutual vortex position [22]. It has been suggested that, testing the properties of the electronic spectrum by means of the heat conductivity measurement, one can directly observe the transition to the multiquantum vortex state in a mesoscopic superconductor [23]. An alternative route is to use STM measurement of local tunneling conductance, which is proportional to the LDOS provided $T \ll T_c$. Thus to provide evidence of multiquantum vortex formation revealed by STM experiments one should find distinctive features of the order parameter structures and LDOS profiles occurring especially in the low temperature regime $T \ll T_c$.

Previously, the low temperature properties of multiquantum vortices have not been investigated much. The results of theoretical studies are known only for a particular case of vortices in clean superconductors when the electronic mean free path is much larger than the coherence length. In this regime the contribution of anomalous branches produces singularities of the order parameter distribution near vortex cores in the limit $T \ll T_c$. In particular, singly quantized vortices feature an anomalous increase of the order parameter slope at the vortex centers, which is known as the Kramer–Pesch effect [24, 25]. The generalization to a multiquantum vortex case was suggested in [26], where it was analytically predicted that a doubly quantized vortex should have a square root singularity of the order parameter distribution $\Delta = \Delta(r)$ in the limit $T \ll T_c$. Although the structures of multiquantum vortices have been calculated self-consistently in the framework of Bogolubov–de Gennes theory the vortex core anomalies have not been discussed [20, 21]. Moreover, multiple anomalous branches of the electronic spectrum have been shown to produce complicated patterns in the LDOS distributions investigated in the framework of Bogolubov–de Gennes theory [20, 21]. Here we employ an alternative approach of the quasiclassical Eilenberger theory [27] to check the predictions of vortex core anomalies and the LDOS patterns in multiquantum vortices in clean superconductors.

Notwithstanding the interesting physics taking place in the clean regime, the experimental realization of STM measurements of multiquantum vortex states was implemented on a Pb superconductor [9, 10] with short mean free path, much smaller than the coherence length. This dirty superconductor is more adequately described within the diffusive approximation of the electronic motion resulting in the Usadel equations for electronic propagators and superconducting order parameters [28]. Singly quantized vortex states in dirty superconductors were investigated in detail [29], and were shown to lack the low temperature singularity of the $\Delta(r)$ distribution, which was smoothed out by the impurity scattering of quasiparticle states. Moreover, the LDOS distribution inside a vortex core does not feature a zero-bias anomaly, since the spectral weight of bound electronic states is distributed smoothly between all energy scales up to the bulk energy gap Δ_0. On the other hand the multiquantum vortex states have not been investigated in the framework of the Usadel theory, nor have the LDOS distributions around multiquantum vortices in dirty superconductors ever been calculated.

It is the goal of the present paper to study both the peculiarities of multiquantum vortex structures, especially at low temperatures, and the distinctive features of electronic LDOS, which would allow unambiguous identification of giant vortices in both clean and dirty regimes. This paper is organized as follows. In section 2 we give an overview of the theoretical framework, namely the quasiclassical Eilenberger theory in clean superconductors and the Usadel equation in the dirty regime. We discuss the results of self-consistent calculations of the order parameter distributions for multiquantum vortex configurations in section 3 and address the LDOS profiles in section 4. We give our conclusions in section 5.

2. Theoretical framework

2.1. Clean limit: Eilenberger formalism

Within quasiclassical approximation [27, 31, 32] the parameters characterizing the Fermi surface are the Fermi velocity V_F and the density of states N_0. We normalize the energies to the critical temperature T_c and length to $\xi_C = \hbar V_F/T_c$. The magnetic field is measured in units $\phi_0/2\pi\xi_C^2$, where $\phi_0 = 2\pi\hbar c/e$ is the magnetic flux quantum. The system of Eilenberger equations for the quasiclassical propagators f, f^+, g reads

$$\begin{aligned} \mathbf{n_p}\,(\nabla + \mathrm{i}\mathbf{A})f + 2\omega f - 2\Delta g = 0, \\ \mathbf{n_p}\,(\nabla - \mathrm{i}\mathbf{A})f^+ - 2\omega f^+ + 2\Delta^* g = 0. \end{aligned} \tag{4}$$

Here $\mathbf{A}$ is a magnetic field vector potential, the vector $\mathbf{n_p}$ parameterizes the Fermi surface and ω is a real quantity which should be taken at the discrete points of Matsubara frequencies $\omega_n = (2n + 1)\pi T$ determined by the temperature T. The quasiclassical propagators obey normalization condition $g^2 + ff^+ = 1$. The self-consistency equation for the order parameter is

$$\Delta(\mathbf{r}) = 2\pi T\Lambda \sum_{n=0}^{N_d} S_F^{-1} \oint_{FS} f(\omega_n, \mathbf{r}, \mathbf{n_p})\, \mathrm{d}^2 S_p \tag{5}$$

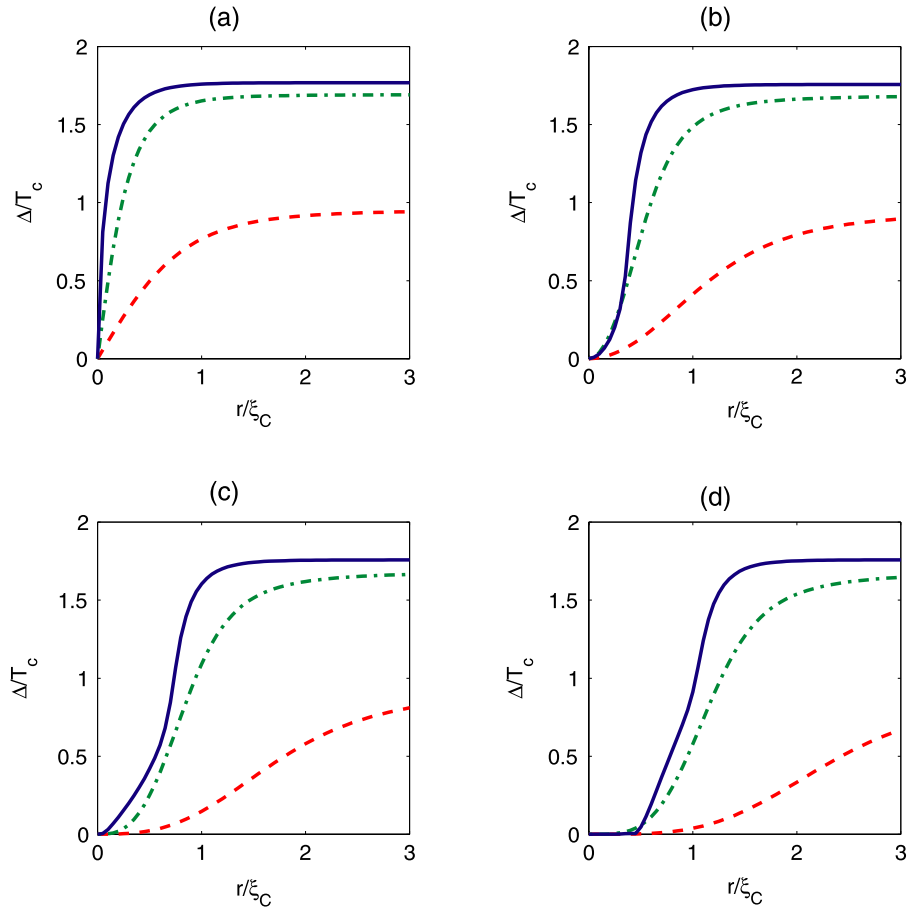

Figure 1. The distribution of the order parameter around vortex cores in a clean superconductor at different temperatures. Panels (a)–(d) correspond to the winding numbers $M = 1, 2, 3, 4$. Blue solid, green dash–dotted and red dashed lines correspond to the temperature $T/T_c = 0.1; 0.5; 0.9$.

where Λ is coupling constant, S_F is a Fermi surface area and the integration is performed over the Fermi surface. Hereafter, to simplify the calculations we assume the Fermi surface to be cylindrical and parameterized by the angle θ_p so that $\mathbf{n_p} = (\cos\theta_p, \sin\theta_p)$. In equation (5), $N_d(T) = \omega_d/(2\pi T)$ is a cutoff at the Debye energy ω_d, which is expressed through physical parameter T_c and Λ as follows:

$$\sum_{n=0}^{N_d(T_c)} \frac{\Lambda}{n+1/2} = 1. \tag{6}$$

The LDOS is expressed through the analytical continuation of the quasiclassical Green's function to the real frequencies

$$N(\mathbf{r}) = N_0 S_F^{-1} \oint_{FS} \mathrm{Re}[g(\omega = -iE + 0, \mathbf{r}, \mathbf{n_p})]\, d^2 S_p. \tag{7}$$

Assuming the vortex line to be oriented along the **z** axis, we choose the following ansatz of the superconducting order parameter corresponding to an axially symmetric vortex bearing M quanta of vorticity $\Delta(x, y) = |\Delta|(r)\, e^{iM\varphi}$, where $r = \sqrt{x^2 + y^2}$ is a distance from the vortex center and $\varphi = \arctan(y/x)$ is a polar angle. Below we neglect the influence of the magnetic field on a vortex structure, which is justified for superconductors with large Ginzburg–Landau parameter.

For numerical treatment of the equations (4) we follow [31, 32] and introduce a Riccati parametrization for the propagators. The essence of this method is a mathematical trick, which allows us to solve two first-order Riccati equations instead of a second-order system of Eilenberger equations. Starting with some reasonable ansatz for the order parameter, the first-order Riccati equations are solved by the standard procedure. Then the corrected order parameter is calculated according to equation (5). The badly converging sum in equation (5) is renormalized in the usual way with the help of equation (6). Then one should take into account only a few terms in the sum (5). For example, $\omega_n < 10T_c$ is enough for the temperature range $T > 0.05T_c$ considered at the present paper. The iteration of this procedure is repeated until convergence of the order parameter is reached with an accuracy $10^{-4}T_c$.

2.2. *Dirty limit: Usadel equations*

In the presence of impurity scattering the Eilenberger equations (4) contain an additional diagonal self-energy term [27]. When the scattering rate exceeds the corresponding energy gap (dirty limit), Eilenberger's theory allows for a significant simplification. In this case quasiclassical Usadel

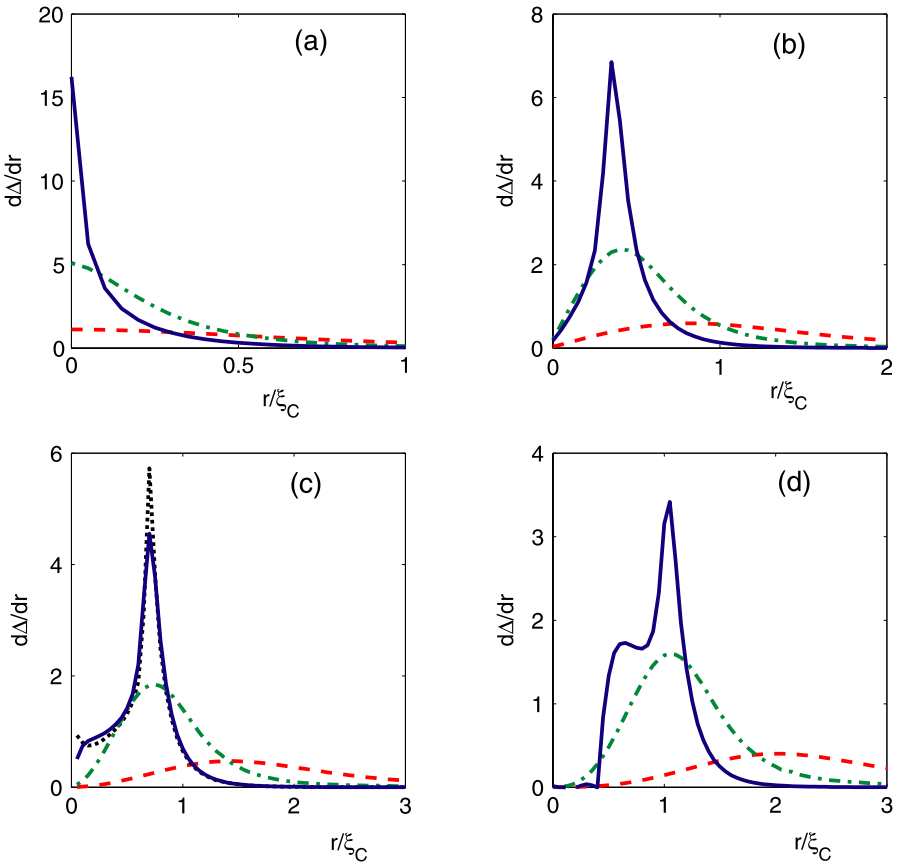

Figure 2. The vortex core anomaly revealed at sharp peaks of the order parameter profile derivative $\mathrm{d}\Delta(r)/\mathrm{d}r$ around vortex cores in a clean superconductor at different temperatures. (a)–(d) Winding numbers $M = 1, 2, 3, 4$ correspondingly. Blue solid, green dash–dotted and red dashed lines correspond to the temperatures $T/T_c = 0.1; 0.5; 0.9$. The dotted black line in (c) is for $T = 0.05T_c$; together with the blue solid curve in (a) it demonstrates the peaked order parameter slope at the vortex center $\mathrm{d}\Delta(r = 0)/\mathrm{d}r$ for odd winding numbers M.

equations [28] are applicable. The structure of singly quantized vortices with $M = \pm 1$ in dirty superconductors was studied extensively in the framework of the Usadel equations [29]

$$\omega F - \left[G(\nabla - \mathrm{i}\mathbf{A})^2 F - F\nabla^2 G\right] = \Delta G \tag{8}$$

where G and F are normal and anomalous quasiclassical Green's functions averaged over the Fermi surface and satisfying the normalization condition $G^2 + F^* F = 1$. To facilitate the analysis, we introduce reduced variables: we use T_c as a unit of energy and $\xi_D = \sqrt{\mathcal{D}/2T_c}$, where $\mathcal{D}$ is a diffusion constant as a unit of length. The Usadel equation (8) is to be supplemented with a self-consistency equation for the order parameter

$$\Delta(\mathbf{r}) = 2\pi T \Lambda \sum_{n=0}^{N_d} F(\omega_n, \mathbf{r}). \tag{9}$$

We again neglect the influence of the magnetic field on a vortex structure. It is convenient to introduce the vector potential in equation (8) corresponding to a pure gauge field which removes the phase of the order parameter

$$\mathbf{A} = M\frac{\mathbf{z} \times \mathbf{r}}{r^2}. \tag{10}$$

Using θ-parametrization [30] ($F = \sin\theta, G = \cos\theta$), the Usadel equation can be rewritten in the form

$$\frac{1}{r}\frac{\mathrm{d}}{\mathrm{d}r}\left(r\frac{\mathrm{d}}{\mathrm{d}r}\theta\right) - \frac{M^2}{2r^2}\sin(2\theta) + (\Delta\cos\theta - \omega\sin\theta) = 0. \tag{11}$$

Performing the renormalization of summation by ω_n in self-consistency equation (9), we need to solve equation (11) for a limited range of frequencies. We take $\omega_n \leq 10T_c$, which allows to obtain very good accuracy. The nonlinear equation (11) was solved iteratively. At first we choose a reasonable initial guess and linearize the equation to find the correction. The corresponding boundary problem for a non-homogeneous second-order linear equation was solved by the sweeping method and the procedure was repeated until convergence was reached. With the help of the obtained solutions of equation (11), we calculated the corrected order parameter (9). We repeated the whole procedure to find the order parameter profile with an accuracy $10^{-4}T_c$.

The LDOS $N(E, r)$, which is accessible in tunneling experiments, can be obtained from $\theta(\omega, r)$ using analytic continuation

$$N(E, r) = \mathrm{Re}\left[\cos\theta(\omega \to -\mathrm{i}E + \delta, r)\right]. \tag{12}$$

To calculate LDOS we solve equation (11) for $\omega = -\mathrm{i}E$. In this case it is in fact a system of two coupled second-order

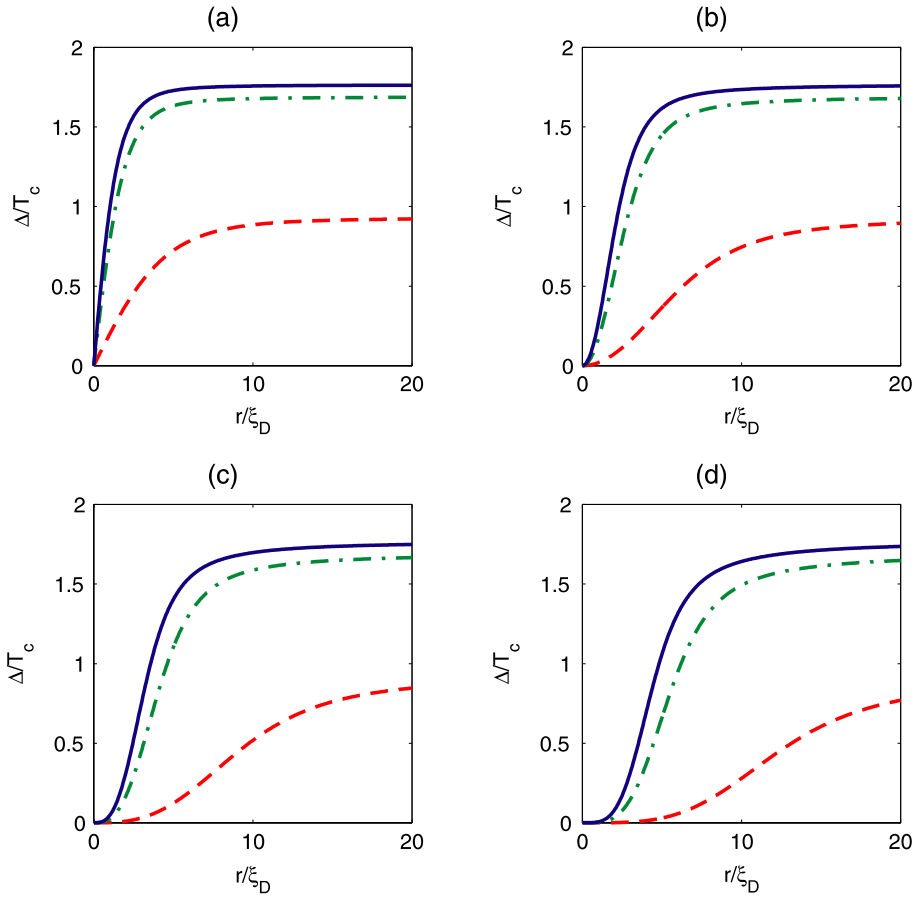

Figure 3. The distribution of the order parameter around the vortex core in a dirty superconductor at different temperatures. (a)–(d) Winding numbers $M = 1, 2, 3, 4$ correspondingly. Blue solid, green dash–dotted and red dashed lines correspond to the temperature $T/T_c = 0.1; 0.5; 0.9$.

equations for the real and imaginary parts of θ. We use the iteration method again by solving repeatedly the linearized system for the corrections of θ. The corresponding boundary problems for second-order linearized equations for $\mathrm{Re}\,\theta$ and $\mathrm{Im}\,\theta$ were solved in turn by the sweeping method.

3. Order parameter structures of multiquantum vortices

To determine the order parameter profiles $\Delta = \Delta(r)$ in multiquantum vortices, we solved numerically the sets of Eilenberger equations (4) and (5) and Usadel equations (9) and (11), which describe the clean and dirty regimes correspondingly. First let us consider the clean regime. The order parameter profiles in vortices with winding numbers $M = 1$–4 are shown in figures 1(a)–(d) for the temperatures $T/T_c = 0.1; 0.5; 0.9$. One can see that at elevated temperatures $T = 0.9T_c$ (red dashed curves) and $T = 0.5T_c$ (green dash–dotted curve) the order parameter follows the Ginzburg–Landau asymptote $\Delta(r) \sim r^M$ at small r.

At low temperature $T = 0.1T_c$ the order parameter distribution is drastically different from the Ginzburg–Landau behavior, as shown by blue solid lines in figure 1. In particular, the singly quantized vortex in figure 1(a) features the Kramer–Pesch effect [24] when the order parameter slope at $r = 0$ grows as $\mathrm{d}\Delta/\mathrm{d}r \sim 1/T$ when $T \to 0$. In the case of multiquantum vortices with $M > 1$, the gapless branches of the electronic spectrum (3) produce anomalies in the vortex core structures [26]. To observe these anomalies we plot in figure 2 the derivatives $\mathrm{d}\Delta(r)/\mathrm{d}r$ obtained self-consistently for the vortex winding numbers $M = 1$–4. In accordance with the analytical consideration [26], the vortex core anomalies result in the singular behavior of $\mathrm{d}\Delta(r)/\mathrm{d}r$ at low temperatures. We find that at $T = 0.1T_c$ in multiquantum vortices with $M > 1$ the calculated dependences $\mathrm{d}\Delta(r)/\mathrm{d}r$ have sharp maxima at finite $r \neq 0$. According to the analytical predictions these maxima originate from the square root singularity of the order parameter which is produced by the contribution of the gapless energy branches of the electronic spectrum [26].

In general, for higher values of winding numbers $M > 1$ in the limit $T \to 0$ one should have $M/2$ singularities of $\mathrm{d}\Delta(r)/\mathrm{d}r$ for even M and $(M + 1)/2$ singularities for odd M. For particular examples of $M = 2, 4$ there are one and two peaks of $\mathrm{d}\Delta/\mathrm{d}r$ at $T = 0.1T_c$ shown by the blue solid line in figures 2(b) and (d). We found that the order parameter of the $M = 3$ vortex has a linear asymptote $\Delta(r) \sim r$ at small r shown in figure 1(c). The slope of this linear dependence grows at decreasing temperature, analogously to the Kramer–Pesch effect in a single-quantum vortex [24]. This

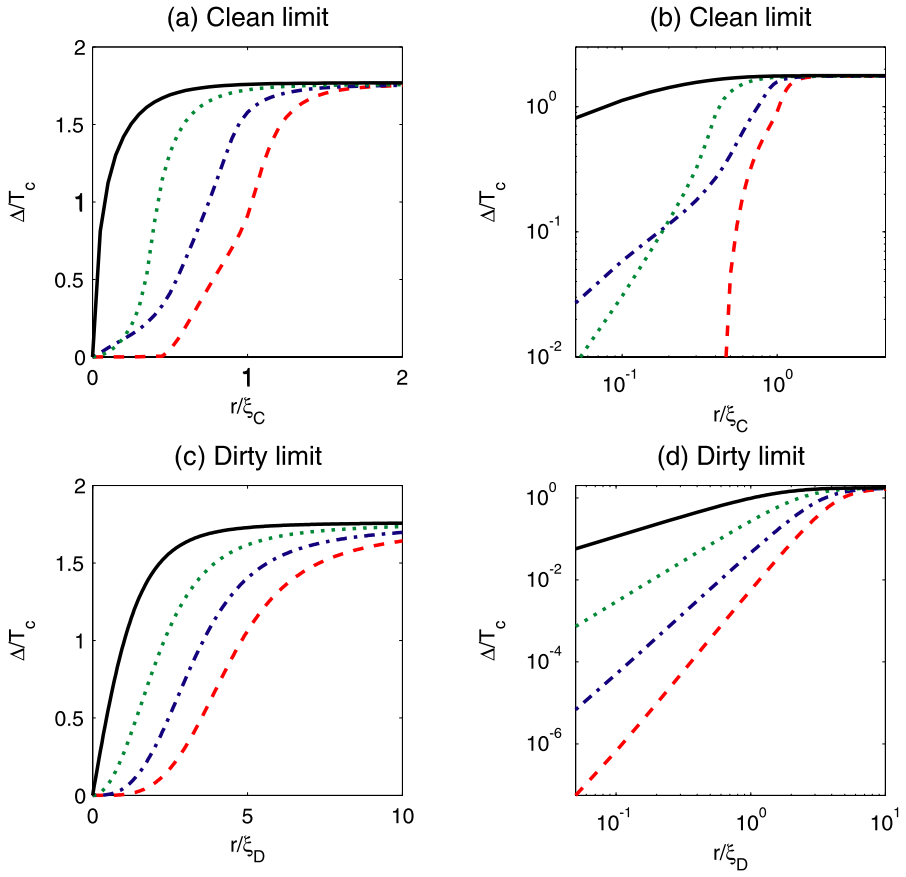

Figure 4. The distribution of the order parameter around the multiquantum vortex core at $T/T_c = 0.1$ in (a) a clean superconductor and (c) a dirty superconductor. The panels (b, d) show the same in logarithmic scale. Black solid, green dotted, blue dash–dotted and red dashed lines correspond to the winding numbers $M = 1, 2, 3, 4$.

behavior is demonstrated by the dotted black line in figure 1(c) corresponding to $T = 0.05T_c$. This effect is featured by all vortices with odd winding numbers originating from the gapless energy branch crossing the Fermi level at $\mu = 0$ in the equation (3).

Next consider the case of a dirty superconductor and calculate the core structures of multiquantum vortices. The results of the calculation are shown in figure 3 for the winding numbers $M = 1$–4 and temperatures $T/T_c = 0.1; 0.5; 0.9$. As expected, vortices in the dirty regime do not feature singularities in the order parameter distribution, in contrast to the clean case considered above.

The comparison of vortex core structures in clean and dirty superconductors at $T/T_c = 0.1$ is presented in figure 4 for the winding numbers $M = 1$–4. To demonstrate the difference between clean and dirty cases we plot the dependences $\Delta = \Delta(r)$ in a logarithmic scale in figures 4(b) and (d) correspondingly. In the dirty case the order parameter has a Ginzburg–Landau power law asymptote $\Delta(r) = \alpha r^M$, which occurs at $r \to 0$ even at very low temperatures $T \ll T_c$. In figures 4(a) and (c) the low temperature behavior $\Delta(r)$ in the clean case is drastically different from the Ginzburg–Landau regime. In particular, the multiquantum vortex with $M = 3$ shown by the blue dash–dotted line in figure 4(a) has a linear asymptote at $r = 0$. The slope of the linear asymptote for $M = 3$ should grow with decreasing temperature, featuring an analog of the Kramer–Pesch effect for multiquantum vortices. Furthermore, the order parameter for the $M = 4$ vortex shown by the red dashed line in figure 4(a) is almost zero in the finite region $r < R_c$, where $R_c \sim \xi_C/2$. This behavior is caused by the dominating contribution of the electronic states (3) to the superconducting order parameter at $r < R_c$. This contribution is zero at $r < \min(\mu_{01}, \mu_{02})/k_F$ in the limit $T \to 0$ [26]. Thus multiquantum vortices with high even winding numbers M are well described by the step-wise vortex core model used previously for the analytical analysis of the vortex core spectrum [19].

4. LDOS profiles of multiquantum vortices

Having in hand the order parameter structures calculated self-consistently in section 3, we calculate the LDOS distributions formed by the electronic states localized at the vortex core. We start with the case of the clean superconductor, which is known to demonstrate peculiar profiles of LDOS originating from multiple energy branches of localized electrons [20, 21]. Here we calculate the LDOS distributions for the winding numbers $M = 1$–4 shown in figure 5. The LDOS plots are similar to that obtained in the framework of Bogolubov–de Gennes theory [20, 21].

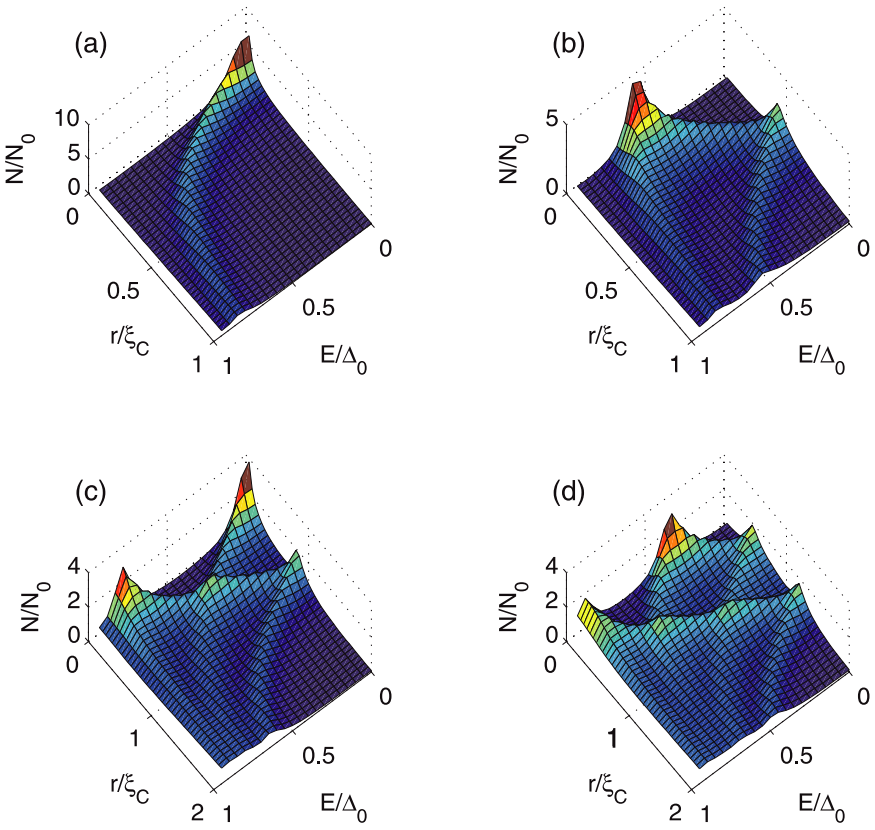

Figure 5. The distribution of the LDOS around vortex cores at $T/T_c = 0.1$ in a clean superconductor as a function of energy and distance from the vortex core $N = N(r, E)$. (a)–(d) Values of vorticity $M = 1, 2, 3, 4$ correspondingly.

Introducing a polar coordinate system (r, φ) and defining the z projection of quasiparticle angular momentum through the impact parameter of the quasiclassical trajectory [23] $\mu = -[\mathbf{r}, \mathbf{k}_F] \cdot \mathbf{z}_0$, the LDOS inside the singly quantized vortex core can be found with the help of equation (2) as follows: $N(E, r) = (k_F/2\pi\xi_C)\int_0^{2\pi} \delta[E - \omega k_F r \sin(\varphi - \theta_p)]\mathrm{d}\theta_p$. Here we evaluate the LDOS summing up over quasiparticle states at the trajectories characterized by the direction of the quasiparticle linear momentum $\mathbf{k_F} = k_F(\cos\theta_p, \sin\theta_p)$. This expression yields a singular behavior of zero energy LDOS at $r > r_0$ [33, 31, 34]: $N(E, r) = 1/(2\pi\omega\sqrt{r^2 - r_0^2}\xi_C) \approx N_0\xi_C/\sqrt{r^2 - r_0^2}$, where $N_0 = (1/2\pi)m/\hbar^2$ is a normal metal LDOS and $r_0 = E/(\omega k_F)$. Thus the LDOS profile of a singly quantized vortex has the ring form, with the radius r_0 being a function of energy. The dependence $N = N(E, r)$ is shown in figure 5(a) for a singly quantized vortex.

In multiquantum vortices the spectrum of low energy states (3) contains several anomalous branches which intersect the Fermi level and contribute to the low energy DOS. The LDOS profile corresponding to the spectrum (3) consists of a set of axially symmetric ring structures [19–21]. Note that for an even winding number the energy branch crossing the Fermi level at $\mu = 0$ (i.e. at zero impact parameter) is absent and, as a result, the LDOS peak at the vortex center disappears. Using the same procedure as for the singly quantized vortices and the spectrum (3), we obtain the LDOS in the form $N(E, r) = \sum_{i=1}^{M} \vartheta(r - r_{0i})/(2\pi\omega_i\sqrt{r^2 - r_{0i}^2}\xi_C)$, where $r_{0i} = (\mu_{0i} + E/\omega_i)/k_F$ and the step function $\vartheta(r) = 0(1)$ at $r < (>)r_{0i}$. At $E = 0$ the spectrum is symmetric, so the LDOS profile has $M/2$ peaks for even M and $(M + 1)/2$ for odd M. At $E \neq 0$ the degeneracy is removed and each peak splits in two, as can be seen from the LDOS plots in figure 5.

Smearing of energy levels due to scattering effects leads to a reduction of the LDOS peak at the vortex center. However, the LDOS peak survives even in the 'dirty' limit, when the mean free path is smaller than the coherence length $l < \xi$. To find the form of the LDOS peak at the vortex core we consider the dirty case described by Usadel equation (11). The LDOS distributions around multiquantum vortices calculated according to equations (11) and (12) are shown in figure 6. The profiles of LDOS at zero energy level $N = N(r)$ in multiquantum vortices $M > 1$ feature a plateau near the vortex center. This is in high contrast to the case of a singly quantized vortex $M = 1$. The cross-sections $N = N(E)$ at different values of distance from the vortex center are shown in figure 7 for $T/T_c = 0.1$ and the winding numbers $M =$ 1–4. These plots clearly demonstrate that with tunneling spectroscopy measurements it is hard to determine the center of the multiquantum vortex core for $M > 2$. Indeed, for $M = 3$ the dependences $N = N(E)$ for $r = 0$ and $r = 2\xi_D$ are very close to each other. For $M = 4$ the same is true up to $r = 3\xi_D$.

In fact, the discussed LDOS plateau occurs due to the very slow spatial dependence of $\delta N(r) = 1 - N(r)/N_0$ at small r, which can be deduced directly from equations (11) and (12).

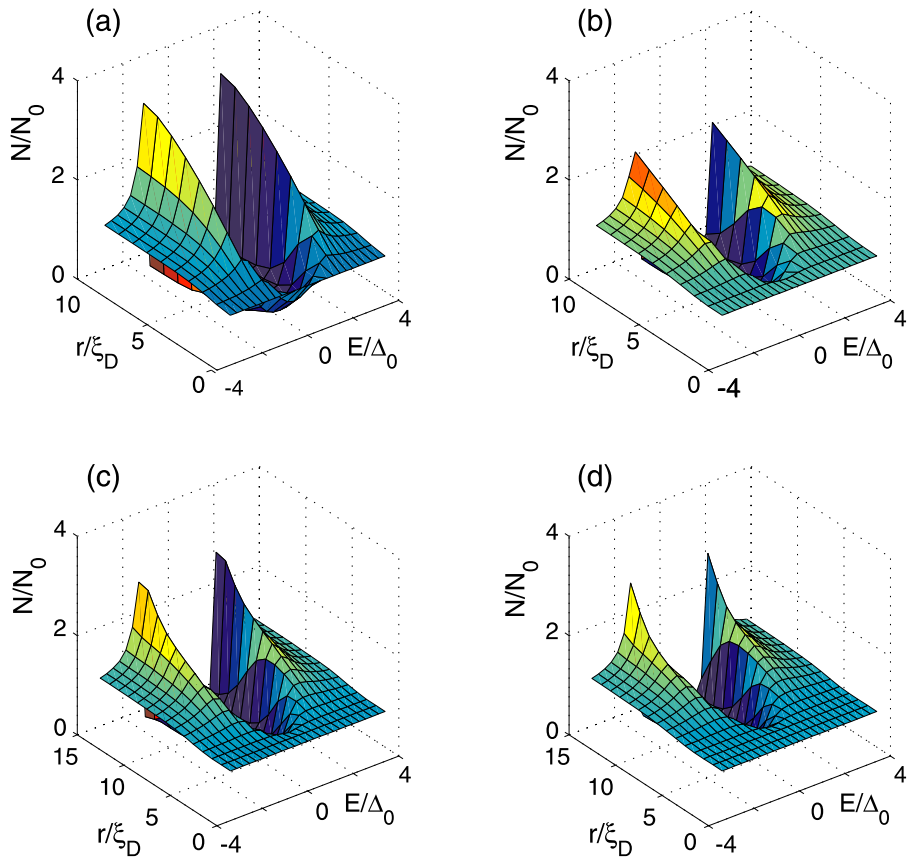

Figure 6. The distributions of LDOS around vortex cores at $T/T_c = 0.1$ in a dirty superconductor as functions of energy and distance from the vortex core $N = N(r, E)$. (a)–(d) Values of winding number $M = 1, 2, 3, 4$.

Indeed, linearizing equation (11) for $\omega = 0$ we obtain

$$\left[\frac{1}{r}\frac{\mathrm{d}}{\mathrm{d}r}\left(r\frac{\mathrm{d}}{\mathrm{d}r}\theta\right) - \frac{M^2}{r^2} + \Delta(r)\right]\theta = 0 \qquad (13)$$

which defines the asymptote $\theta(r) = \alpha r^M$. Next equation (12) yields the LDOS deviation $\delta N = \theta^2/2 = \alpha^2 r^{2M}/2$. This analytical asymptote perfectly agrees with the numerical results, which can be seen from the logarithmic scale plot of $N(r)$ in figure 6(b). An interesting feature of such LDOS plateaus is that they survive at distances comparable to the size of the multiquantum vortex core, which is much larger than the coherence length ξ_D. This is we find that the size of the plateau shown in figure 8 is approximately given by $R_p = M\xi_D/2$ for $M > 1$.

5. Conclusion

To summarize, we have calculated self-consistently in the framework of quasiclassical Eilenberger theory the order parameter structures of multiquantum vortices together with the local density of electronic states in both clean and dirty superconductors. We have found that at temperatures near T_c the order parameter profiles of vortices are qualitatively similar in clean and dirty regimes (compare the dependences $\Delta(r)$ for $T = 0.9T_c$ shown by the red dashed curves in figures 1 and 3 for clean and dirty cases correspondingly). In this temperature regime the order parameter asymptote at $r \to 0$ is determined by the power law $\Delta(r) = \alpha r^M$, which is consistent with the result of Ginzburg–Landau theory valid at $|T/T_c - 1| \ll 1$.

On the other hand, in the low temperature limit $T = 0.1T_c$ vortices in a clean superconductor demonstrate anomalies in the order parameter distribution—the singularities of the derivative $\mathrm{d}\Delta/\mathrm{d}r$ predicted in [26] and shown in figure 2. Such singularities occur due to the contribution of gapless electronic spectral branches to the order parameter. The singular behavior of $\mathrm{d}\Delta/\mathrm{d}r$ in multiquantum vortices is analogous to the Kramer–Pesch effect [24] occurring for the singly quantized vortices $M = 1$ which have steep order parameter slope $\mathrm{d}\Delta/\mathrm{d}r(r = 0) \sim 1/T$ at $T \to 0$. In dirty superconductors the asymptote $\Delta(r \to 0)$ at the vortex core obeys the Ginzburg–Landau power law behavior even at low temperature $T = 0.1T_c$, which is clearly demonstrated in logarithmic scale plots in figure 4(d).

In the framework of quasiclassical theory, we calculated the LDOS distributions in multiquantum vortices with winding numbers $M = 1$–4. The LDOS profiles in the clean regime are similar to that obtained previously with the help of Bogolubov–de Gennes theory [20, 21]. Most importantly, we determined the LDOS profiles in the dirty regime which directly correspond to the modern experiments on scanning tunneling microscopy of multiquantum vortices in mesoscopic superconductors. The zero energy LDOS profile near the vortex center is shown to be $N(r)/N_0 = 1 - \alpha r^{2M}$,

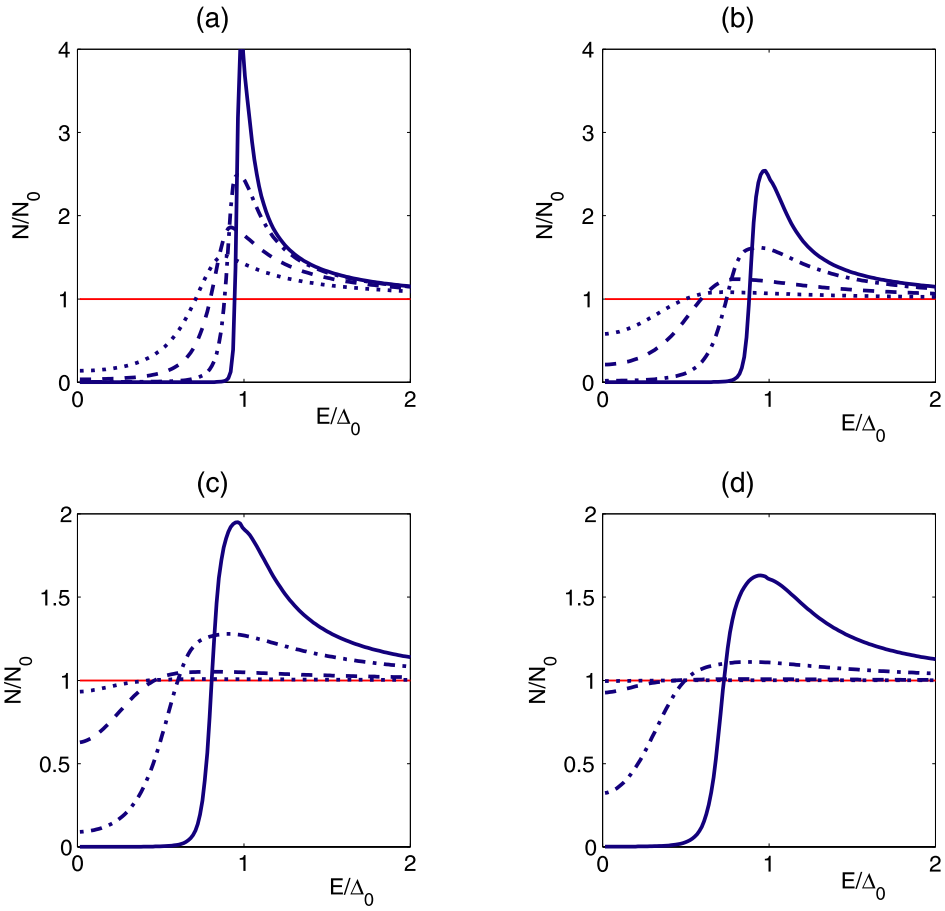

Figure 7. The cross-sections $N = N(E)$ at different values of distance from the vortex center r in a dirty superconductor at $T/T_c = 0.1$. (a)–(d) Values of winding number $M = 1, 2, 3, 4$. Blue dotted, dash–dotted, dashed and solid lines correspond to the distances $r/\xi_D = 2; 3; 5; 10$. The thin solid red line indicates the flat LDOS at the vortex center $r = 0$.

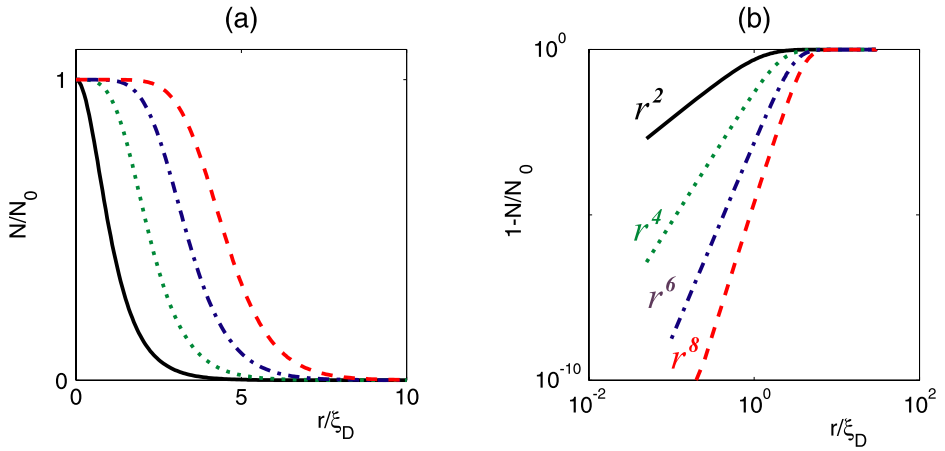

Figure 8. (a) The LDOS profiles for zero energy $E = 0$ around vortices at $T/T_c = 0.1$ in a dirty superconductor as a function of the distance from the vortex center $N = N(r)$. (b) The logarithmic plot of $\delta N(r) = 1 - N(r)/N_0$, demonstrating the power law asymptote $\delta N(r) \sim r^{2M}$ at $r \to 0$. Black solid, green dotted, blue dash–dotted and red dashed lines correspond to the winding numbers $M = 1, 2, 3, 4$.

which holds with good accuracy at $r < M\xi_D/2$. Thus for the values of $M > 2$ the LDOS profile is almost flat in the sizable region near the vortex center $r < M\xi_D/2$ (see figure 8). Such an LDOS plateau can be considered as a hallmark of multiquantum vortex formation revealed by STM in dirty mesoscopic superconductors [9, 10].

Acknowledgments

This work was supported, in part, by the Russian Foundation for Basic Research grant No 13-02-01011 and the Russian President Foundation (SP-6811.2013.5).

References

[1] Schweigert V A, Peeters F M and Deo P S 1998 *Phys. Rev. Lett.* **81** 2783
Chibotaru L F, Ceulemans A, Bruyndoncx V and Moshchalkov V V 2000 *Nature* **408** 833

[2] Geim A K, Dubonos S V, Palacios J J, Grigorieva I V, Henini M and Schermer J J 2000 *Phys. Rev. Lett.* **85** 1528

[3] Palacios J J 1998 *Phys. Rev.* B **58** R5948

[4] Chibotaru L F, Ceulemans A, Bruyndoncx V and Moshchalkov V V 2001 *Phys. Rev. Lett.* **86** 1323

[5] Kanda A, Baelus B J, Peeters F M, Kadowaki K and Ootuka Y 2004 *Phys. Rev. Lett.* **93** 257002

[6] Grigorieva I V *et al* 2007 *Phys. Rev. Lett.* **99** 147003

[7] Geim A K *et al* 1997 *Nature* **390** 259

[8] Kramer R B G, Silhanek A V, Van de Vondel J, Raes B and Moshchalkov V V 2009 *Phys. Rev. Lett.* **103** 067007

[9] Cren T, Serrier-Garcia L, Debontridder F and Roditchev D 2011 *Phys. Rev. Lett.* **107** 097202

[10] Cren T, Fokin D, Debontridder F, Dubost V and Roditchev D 2009 *Phys. Rev. Lett.* **102** 127005

[11] Hess H F, Robinson R B, Dynes R C, Valles J M Jr and Waszczak J V 1989 *Phys. Rev. Lett.* **62** 214
Hess H F, Robinson R B and Waszczak J V 1990 *Phys. Rev. Lett.* **64** 2711

[12] Hoogenboom B W, Kugler M, Revaz B, Maggio-Aprile I, Fischer O and Renner Ch 2000 *Phys. Rev.* B **62** 9179

[13] Kohen A, Proslier Th, Cren T, Noat Y, Sacks W, Berger H and Roditchev D 2006 *Phys. Rev. Lett.* **97** 027001

[14] Guillamon I, Suderow H, Vieira S, Cario L, Diener P and Rodiere P 2008 *Phys. Rev. Lett.* **101** 166407

[15] Fischer O, Kugler M, Maggio-Aprile I, Berthod C and Renner C 2007 *Rev. Mod. Phys.* **79** 353

[16] Caroli C, de Gennes P G and Matricon J 1964 *Phys. Lett.* **9** 307

[17] Volovik G E 1996 *JETP Lett.* **63** 729

[18] Tanaka Y, Hasegawa A and Takayanagi H 1993 *Solid State Commun.* **85** 321
Tanaka Y, Kashiwaya S and Takayanagi H 1995 *Japan. J. Appl. Phys.* **34** 4566
Rainer D, Sauls J A and Waxman D 1996 *Phys. Rev.* B **54** 10094

[19] Mel'nikov A S and Vinokur V M 2002 *Nature* **415** 60
Mel'nikov A S and Vinokur V M 2002 *Phys. Rev.* B **65** 224514

[20] Tanaka K, Robel I and Janko B 2002 *Proc. Natl Acad. Sci.* **99** 5233

[21] Virtanen S M M and Salomaa M M 1999 *Phys. Rev.* B **60** 14581
Virtanen S M M and Salomaa M M 2000 *Physica* B **284** 741

[22] Mel'nikov A S, Ryzhov D A and Silaev M A 2009 *Phys. Rev.* B **79** 134521

[23] Mel'nikov A S, Ryzhov D A and Silaev M A 2008 *Phys. Rev.* B **78** 064513

[24] Pesch W and Kramer L 1973 *J. Low Temp. Phys.* **15** 367

[25] Gygi F and Schluter M 1991 *Phys. Rev.* B **43** 7609

[26] Volovik G E 1993 *JETP Lett.* **58** 455

[27] Eilenberger G 1968 *Z. Phys.* **214** 195

[28] Usadel K 1970 *Phys. Rev. Lett.* **25** 507
Usadel K 1971 *Phys. Rev.* B **4** 99

[29] Kramer L, Pesch W and Watts-Tobin R J 1974 *J. Low Temp. Phys.* **17** 71

[30] Kramer L, Pesch W and Watts-Tobin R J 1974 *J. Low Temp. Phys.* **14** 29

[31] Schopohl N and Maki K 1995 *Phys. Rev.* B **52** 490

[32] Schopohl N 1998 arXiv:9804064

[33] Ullah S, Dorsey A T and Buchholtz L J 1990 *Phys. Rev.* B **42** 9950

[34] Hayashi N, Ichioka M and Machida K 1996 *Phys. Rev. Lett.* **77** 4074
Hayashi N, Ichioka M and Machida K 1997 *Phys. Rev.* B **56** 9052